Journal of Applied Polymer Science

Study of crystallization behavior of neat poly(vinylidene fluoride) and transcrystallization in carbon fiber/poly(vinylidene fluoride) composite under a temperature gradient

Shengnan Zhang,[1] Hai Wang,[2] Duigong Xu,[3] Wenxiao Yang,[1] Ping Tang,[1] Yuezhen Bin[1]

[1]Department of Polymer Science and Engineering, Dalian University of Technology, Dalian, 116024, China

[2]Department of Future Industry-Oriented Basic Science and Materials, Toyota Technological Institute, Nagoya, 4618511, Japan

[3]China Academy of Engineering Physics, Mianyang, 621900, China

Correspondence to: Y. Bin (E-mail: binyz@dlut.edu.cn)

ABSTRACT: The crystallization behavior of poly(vinylidene fluoride) (PVDF) and transcrystallization in carbon fiber (CF)/PVDF composite were investigated under a temperature gradient. The crystallization temperature (T_c) was controlled in the range of 110–180 °C. For neat PVDF, the results showed that exclusive γ phase formed at T_c above 164 °C, but coexisted with α phase at T_c ranging from 137 to 160 °C. The promotion of γ phase to nucleation of α phase at low T_c was observed for the first time. For CF/PVDF composite, a cylindrical transcrystalline (TC) layer formed on the surface of CF when T_c was between 137 and 172 °C. The TC layer was exclusively composed of γ phase at T_c above 164 °C. The hybrid nucleation was dominated by γ phase though some α phase nuclei emerged on the surface of CF when T_c was in the range of 144–160 °C. As T_c decreased, competition between the hybrid nucleation of α and γ phase became more intense. The γ phase nuclei was soon circumscribed by the rapidly developed α phase when T_c was below 144 °C. Furthermore, some α phase nuclei were induced at the surface of the γ phase TC layer, and developed into α phase TC layer when T_c was in the range of 146–156 °C, which resulted in a doubled TC layer of α and γ phase at the interface of the composite. © 2016 Wiley Periodicals, Inc. J. Appl. Polym. Sci. **2016**, *133*, 43605.

KEYWORDS: composites; crystallization; fibers; morphology; surfaces and interfaces

Received 30 September 2015; accepted 4 March 2016

DOI: 10.1002/app.43605

INTRODUCTION

Poly(vinylidene fluoride) (PVDF) is an attractive material due to its strong piezoelectricity and pyroelectricity.[1] PVDF has four crystalline phases at least, including α (Form II), β (Form I), γ (Form III), and δ (Form IV).[1–5] The α and γ phases could be obtained when PVDF crystallized from the melt.[6] Meanwhile, α and β phases transformed to γ phase under high temperature annealing.[6] Hence, it is of great importance to study the crystallization behavior of PVDF at different temperatures. It is well known that the addition of fillers is an effective way to control the supermolecular structure and to improve the physical properties of polymer materials. Carbon fiber (CF) has been one of the most popular fillers during the past decades because of its outstanding mechanical and electrical properties.[7] Thus, CF is an attractive candidate to widen the applications of PVDF. CF has been used as reinforcement or functional filler to fabricate conductive PVDF composites.[8,9] Unfortunately, the obvious differences between CF surface characteristic and polymer matrix resulted in poor interface interaction.

In fiber-filled semicrystalline polymer composites, the phenomenon of transcrystallinity could be observed at the interface of polymer matrix and fiber if the fiber could initiate high density of hybrid nucleation on its surface.[10–13] In this case, spherulite growth is restricted to one direction, which is perpendicular to the long axis of the fiber. As an interfacial structure with cylindrical shape, transcrystalline (TC) morphology has been drawing more and more attention because it has the potential to enhance the interfacial interaction between polymer matrix and fillers.[14] Karger et al. reported the enhanced interfacial adhesion strength due to the transcrystallized isotactic polypropylene (*i*PP) layer.[15,16] Cho et al. found the dramastically increased interfacial interfaction between trancrystallized *i*PP layer and silicon substrate.[17] Xu et al. studied the transcrystallization in poly(lactic acid)/natural fiber and proved that the transcrystallinity did improve the interfacial shear strength of the composite.[18] Many factors, such as surface chemical and physical characteristics of the fillers, molecular weight, chain conformation and functional groups of polymer matrix, and various kinds of external fields, have effects on transcrystallization.[14] Varga and

Karger–Kocsis studied the crystallization behavior of *i*PP at the interfacial of *i*PP and glass fiber composites. They discussed the effects of crystallization temperature, molecular orientation and pulling temperature on the formation of transcrystallized or spherulitic *i*PP in details.[19,20] As for a given polymer composite system, the crystallization temperature (T_c) has a significant influence on the TC morphology and transcrystallizaiton kinetics.[21] Therefore, a homemade temperature gradient (T-gradient) hot stage was employed for the first time to study the influence of T_c on the transcrystallization behavior at the interface of CF/PVDF composite in this work. T-gradient hot stage provides a controlled range of temperatures that involves continuous variation. As a kind of high-throughput screening method, it improves the efficiency and accuracy of experiment at the same time.

The primary purpose of this study was to investigate the transcrytallization behavior of PVDF at the interface of CF/PVDF composites, in particularly, the impact of varying T_c on the transcrystalline morphology and trancrystallization kinetics. It was also necessary to clarify the differences between the transcrystallized PVDF and spherulitic PVDF at different T_c on crystalline morphology and crystallization kinetics by comparing the crystallization behavior of CF/FVDF composite and neat-PVDF.

EXPERIMENTAL

Construction of Temperature Gradient

Figure 1(a) shows the schematic of the T-gradient hot stage employed in this study. Copper plate was selected as the heat conducting medium to form a continuous T-gradient from one side to the other side. The endpoint temperatures of the stage were adjusted by a heater and cooler. To minimize convective heat transfer with air, the stage was sealed with glass cover and vacuum pump. The distance between the temperature measurement sites was 1 cm. The first site on the left was set as 0 cm, so the tenth site was 9 cm away from the first site. The information detailing the preparation of the T-gradient hot stage and the calibration of surface temperature was depicted in our previous work.[22] The temperature range of the T-gradient was 110–180 °C that covered the melting poing (T_m) of PVDF and designated T_cs in this work. Figure 1(b) presents the surface temperatures of the T-gradient stage at different positions.

Preparation of PVDF Film and CF/PVDF Composite Film

PVDF (Solef 1015, melt flow index of 2.6 to 4.8 g/ 10 min, 230 °C/21.6 kg) purchased from Solvay specialty polymers was dissolved in cosolvent of *N*,*N*-dimethyl formamide (DMF) and acetone (volume ratio 2:1). The concentration of the solution was 4% (w/w). PAN-based CF with a filament diameter of 5 μm was purchased from Jilin Chemical Group, China National Petroleum Corporation. The purchased CF was desized and ultrasonically dispersed in acetone to remove sizing agent. Then single CF fiber was arranged paralleled to each other with an interval of 2 mm and fixed on the slide glass. PVDF solution was cast on the slide glass and kept at 80 °C for 1 h to evaporate solvent. Finally, thin film of CF/PVDF composite with a thickness of ca. 10 μm was obtained. A schematic of the CF/PVDF composite film is shown in Figure 1(c). PVDF film was made under the same condition as CF/PVDF composite film. A thermogravimetric analysis (TGA) was carried out for the as-cast PVDF and CF/PVDF thin film by using the TA Q600 thermogravimetric analyzer. No weight loss was observed at the temperature around 150 °C, indicating that no residual DMF solvent in the film.

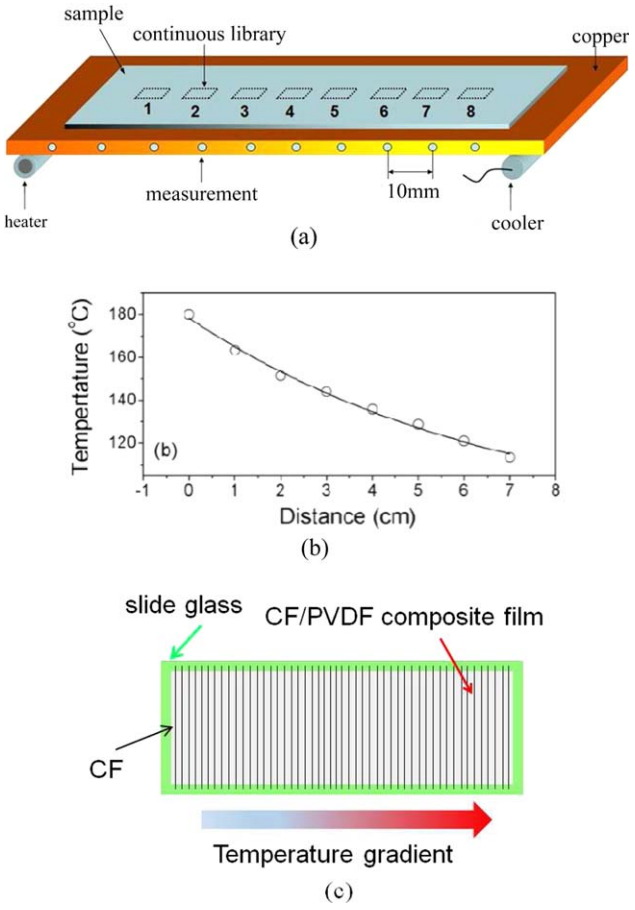

Figure 1. (a) The schematic of T-gradient hot stage, (b) surface temperatures of the T-gradient hot stage at different positions, and (c) schematic of CF/PVDF composite film on a slide glass. [Color figure can be viewed in the online issue, which is available at wileyonlinelibrary.com.]

Isothermal Crystallization on the T-gradient

Thin films of PVDF and CF/PVDF composite on slide glass were heated at 220 °C for 7 min to remove heat history. Then they were quickly transferred to the preheated T-gradient hot stage and crystallized isothermally. Neat PVDF was crystallized for 8 h, and CF/PVDF composite for 4 h. Finally, the films were quenched by ice water to reduce cold crystallization during cooling. Because subsamples of the films were crystallized at different T_cs, a T_c-crystal morphology library was built. In this way, the dependence of crystallization behavior of neat PVDF and transcrystallization behavior of CF/PVDF composite on T_c can be observed and compared very clearly.

Polarized Microscopy

The crystal morphology of PVDF and CF/PVDF after isothermal crystallization was observed by polarized-light optical microscope (POM) (Optiphot2-POL, Nikon, Japan). In additon, the isothermal crystallization of neat PVDF and transcrystallization of

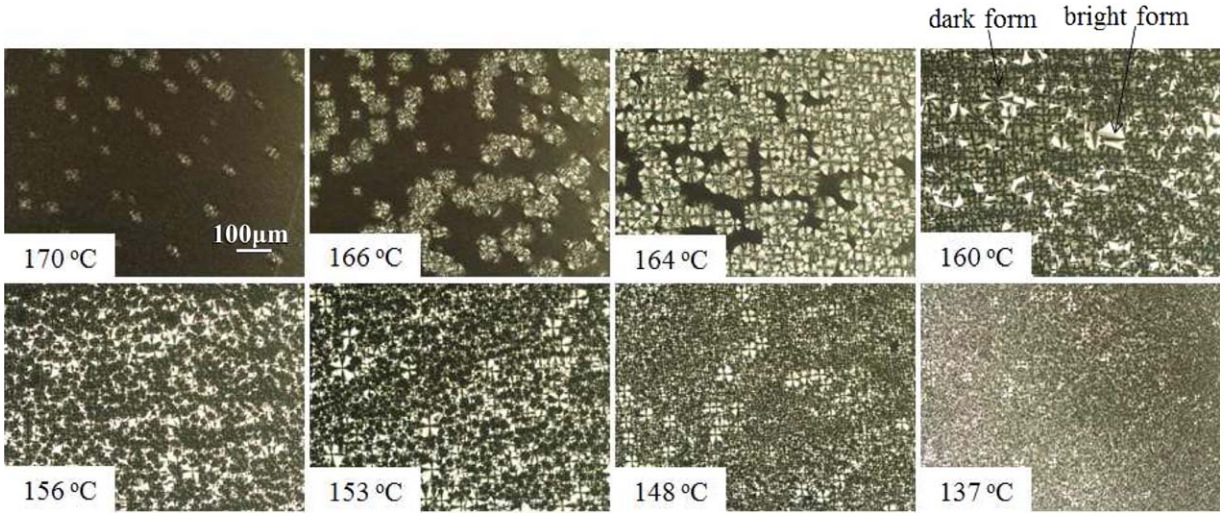

Figure 2. The selected POM images from the T_c-crystal morphology library of neat PVDF film after isothermal crystallization for 8 h. [Color figure can be viewed in the online issue, which is available at wileyonlinelibrary.com.]

CF/PVDF were recorded by the POM equipped with a heating-cooling stage and temperature controller. The samples for isothermal crystallization were heated at 220 °C for 7 min, and then quickly quenched to 137, 145, 150, 155, and 160 °C, respectively. The growth rate (G) of PVDF spherulites or TC layers was calculated according to the eq. (1):

$$G = \frac{R_2 - R_1}{t_1 - t_2} \quad (1)$$

where R_1 and R_2 are the radii of spherulites or thickness of TC layers at crystallization time t_1 and t_2, respectively.

Micro-Raman Spectroscopy

Different crystalline phases formed during the isothermal crystallization of the neat PVDF melt were confirmed by a micro-Raman spectroscopy (Thermo scientific, DXR Raman Microscope, +CCD detector, $\lambda = 532$ nm). The mirco-Raman scan was conducted for selected spherulites of the neat PVDF crystallized at different temperatures. Then, the TC phases formed at 150 °C were also invetigated by the micro-Raman spectroscopy. The scan of the TC layer was performed along a 90 μm (5–95 μm away from the surface of CF) line perpendicular to the long axis of the CF (or paralleled to the growth direction of PVDF transcrystalline phase) with a step size of 5 μm.

Fourier Transform Infrared

To investigate the dependence of crystalline phase contents on T_c, subsamples of neat PVDF crystallized at 137, 148, 153, and 160 °C were selected from the T_c-crystal morphology library to perform the Fourier transform Infrared (FTIR) (Thermo scientific, NICOLET 6700) measurement.

Differetial Scanning Calorimeter

Subsamples of neat PVDF crystallized at 137, 148, 156, 160, and 164 °C were selected from the T_c-crystal morphology library to conduct the differetial scanning calorimeter (DSC) (TA DSC Q1000) measurement. All the samples were heated from room temperautre to 220 °C at a rate of 5 °C min^{-1} under nitrogen gas atmosphere.

RESULTS AND DISCUSSION

Crystal Morphology of Neat PVDF

Figure 2 includes selected POM images of neat PVDF film after isothermal crystallization for 8 h on the T-gradient stage. It could be seen that neat dark-form spherulites formed when T_c was in the range of 164–170 °C. As T_c decreased to 160 °C, another kind of spherulites formed, which was brighter than the ones formed above 160 °C. Figure 3 shows the morphology of the dark and bright spherulites of PVDF. According to Silvar *et al.*,[23] the dark spherulites could be identified as γ phase, and the bright spherulite as α phase. The two crystalline forms were confirmed in the next section.

Figure 2 suggested that the total nuclei density of the two types of spherulites increased as T_c decreased. The nucleation of dark spherulites was dominant when T_c was high (above 160 °C). However, nuclei density of bright spherulites increased as T_c decreased. In other words, the nucleation ability of the bright-form crystalline phase was much weaker than the dark one at

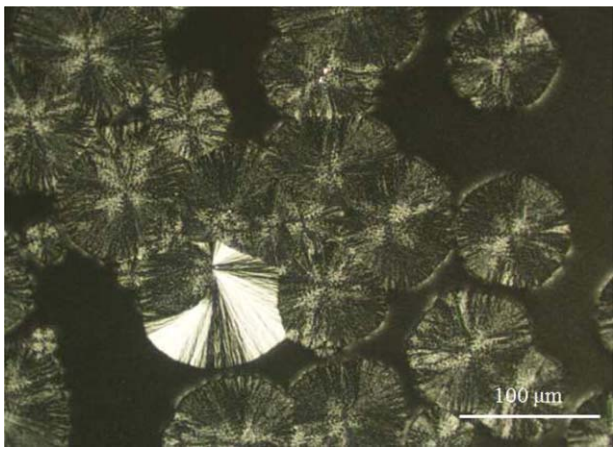

Figure 3. The morphology of dark and bright spherulites of PVDF after isothermal crystallization for 4 h at 160 °C. [Color figure can be viewed in the online issue, which is available at wileyonlinelibrary.com.]

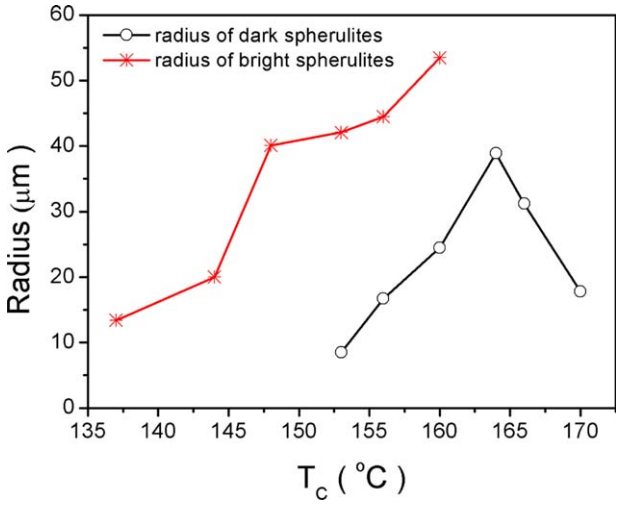

Figure 4. The radii of bright- and dark-form spherulites of PVDF crystallized isothermally at different T_cs for 8 h. [Color figure can be viewed in the online issue, which is available at wileyonlinelibrary.com.]

high T_c, but it increased gradually with the decreasing T_c. Figure 4 shows the radii of bright- and dark-form spherulites of PVDF crystallized isothermally on the T-gradient for 8 h. The radii of the bright-form spherulites were about 30 μm larger than that of the dark-form ones at the same T_c.

To confirm the crystalline phases of the bright and dark spherulites, micro-Raman measurement was performed by focusing the micro-Raman beam on the dark and bright spherulites respectively. A comparison of the micro-Raman spectra of the bright and dark spherulites are shown in Figure 5, including the low Raman shift region (Figure 5, left) and high Raman shift region (Figure 5, right). The bright spherulite (red line) shows characteristic Raman bands at 283 cm^{-1} [δ(CCC)], 410 cm^{-1} [γ (CF_2), γ (CH_2)], 535 cm^{-1} [$\delta(CF_2)$], 610 cm^{-1} [$\delta(CF_2)$], 1058 cm^{-1} [$\nu_s(CF_2)$, $\omega(CH_2)$], and 1198 cm^{-1} [$\nu_s(CF_2)$, $\tau(CH_2)$], which is correspondent with the α crystalline phase.[24–26] The dark spherulite (black line) exhibited characteristic Raman bands at 512 cm^{-1} [$\delta(CF_2)$], 812 cm^{-1} [$\gamma(CH_2)$], 1135 cm^{-1} [ν(CC), $\omega(CF_2)$] and 1234 cm^{-1} [$\nu_{as}(CF_2)$, $\gamma(CF_2)$], which corresponds to γ crystalline phase.[24–26]

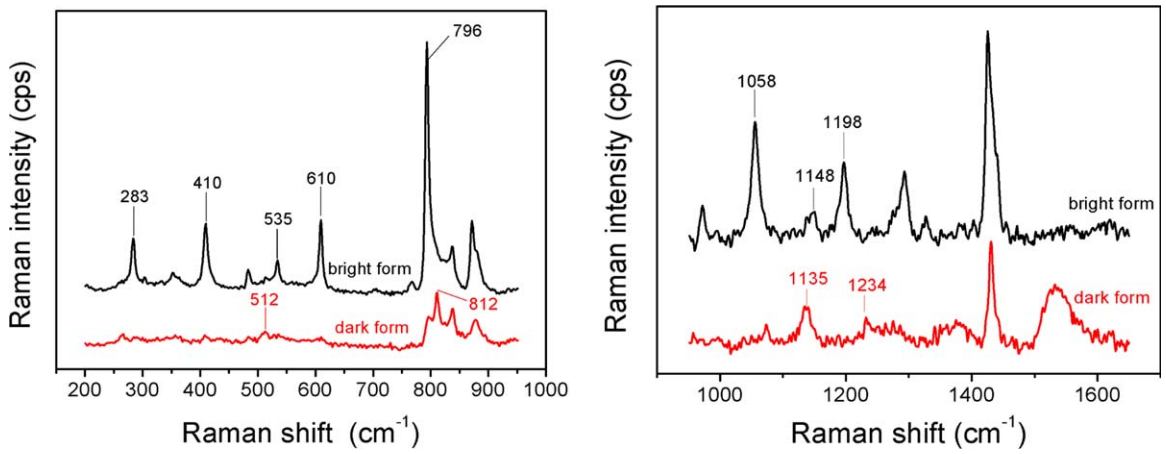

Figure 5. The micro-Raman spectra of a single bright and dark spherulite of PVDF in low Raman shift region (left) and high Raman shift region (right). [Color figure can be viewed in the online issue, which is available at wileyonlinelibrary.com.]

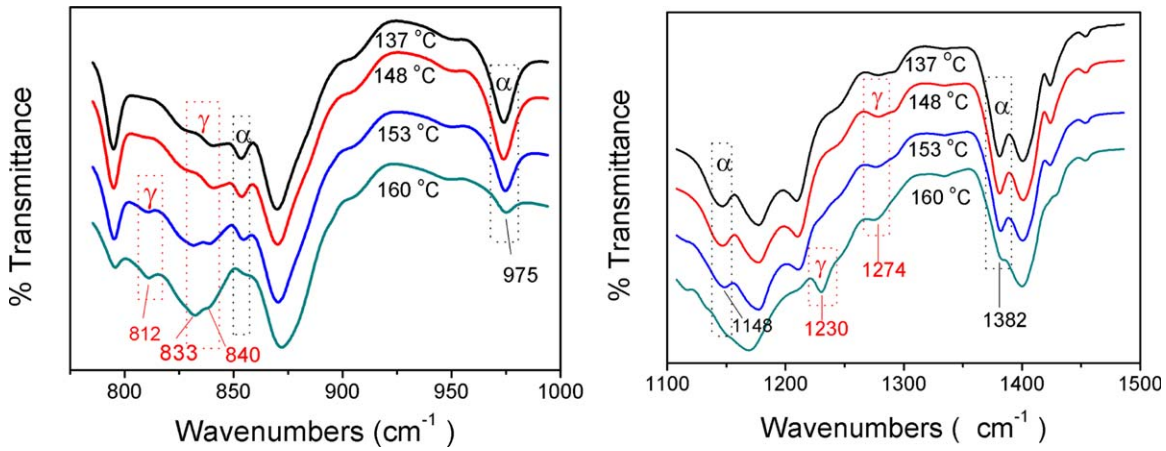

Figure 6. The FTIR spectra of PVDF crystallized isothermally at different temperatures for 8 h. [Color figure can be viewed in the online issue, which is available at wileyonlinelibrary.com.]

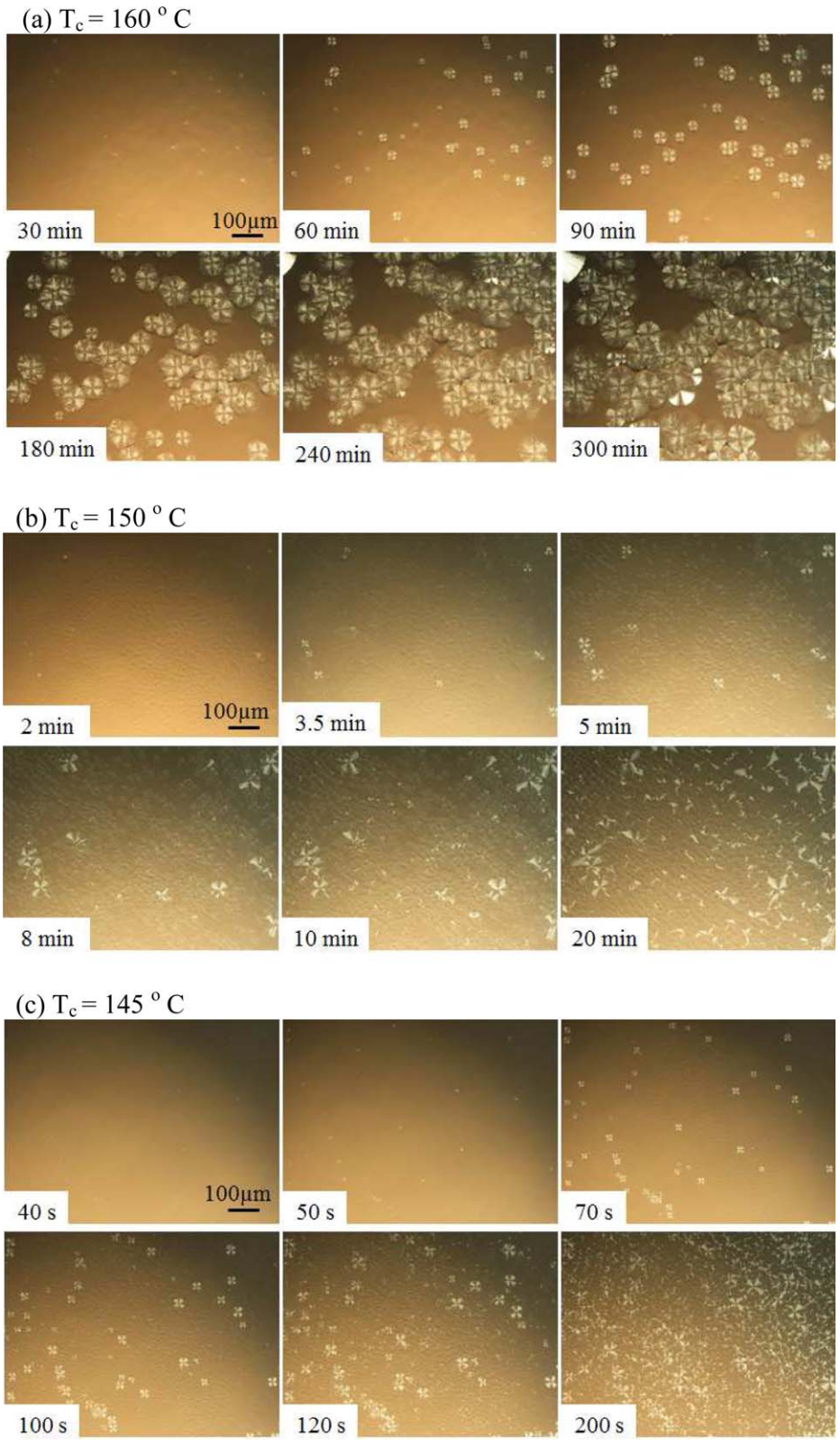

Figure 7. The selected POM images of during the isothermal crystallization of PVDF at different temperatures. [Color figure can be viewed in the online issue, which is available at wileyonlinelibrary.com.]

The FTIR measurement of neat PVDF crystallized at 137, 148, 153, and 160 °C could also be used to confirm the crystalline phase of the bright and dark spherulites as shown in Figure 6. At T_c = 137 °C, the FTIR spectrum shows mainly the characteristic band of the α crystalline phase at 975 cm^{-1} ($\tau(CH_2)$), 1148 cm^{-1} (ν_s(CF2), ν_a(CC)), 1382 cm^{-1} ($\delta(CH_2)$, $\omega(CH_2)$),

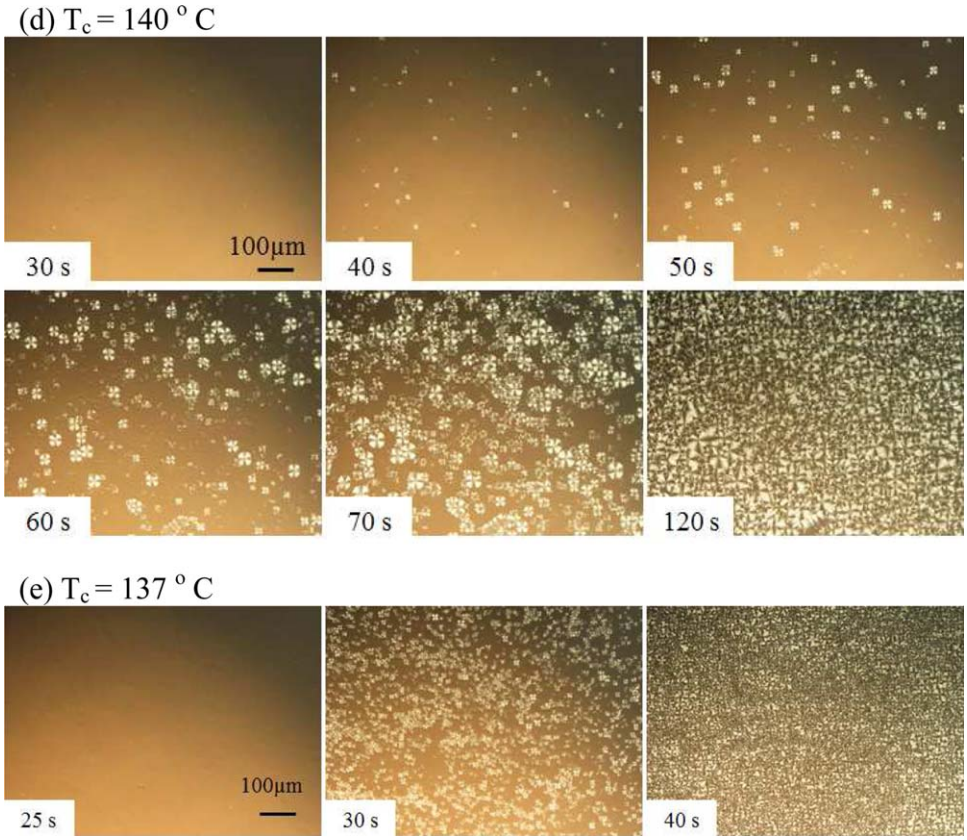

Figure 7. (Continued). [Color figure can be viewed in the online issue, which is available at wileyonlinelibrary.com.]

which was related with the dominant dark spherulite. At $T_c = 160\,^{\circ}C$, a series of the FTIR bands of the γ crystalline phase was observed at 812, 833, 840 cm^{-1} ($\gamma(CH_2)$), 1230 and 1274 cm^{-1} ($\nu_s(CF_2)$, $\nu_s(CC)$), which was correspondent with the bright spherulite.[24–26] Therefore, the bright spherulite was confirmed to be the γ crystalline phase, and the dark spherulite was the α crystalline phase. As demonstrated in Figure 6, the content of γ phase decreased as T_c decreased according to the intensity change of the γ phase charateristic bands. This tendency was in agreement with POM observation in the T_c-crystal morphology library.

Crystallization Kinetics of Neat PVDF

Neat PVDF films of 10 μm thickness were melt at 220 °C for 7 min, and then cooled rapidly to a series of preset temperatures (i.e., 160, 155, 150, 145, 140, and 137 °C), and isothermally crystallized at those temperatures. Figure 7 shows the POM images of isothermal crystallization of neat PVDF at different T_cs, from which the formation of α and γ phase spherulites is seen clearly. As suggested in Figure 7, the nucleation rate of γ phase was much higher than that of α phase at 160 and 150 °C. The crystallization of γ phase was prevailing at high T_c. As T_c decreased, the nucleation rate of α phase increased, which

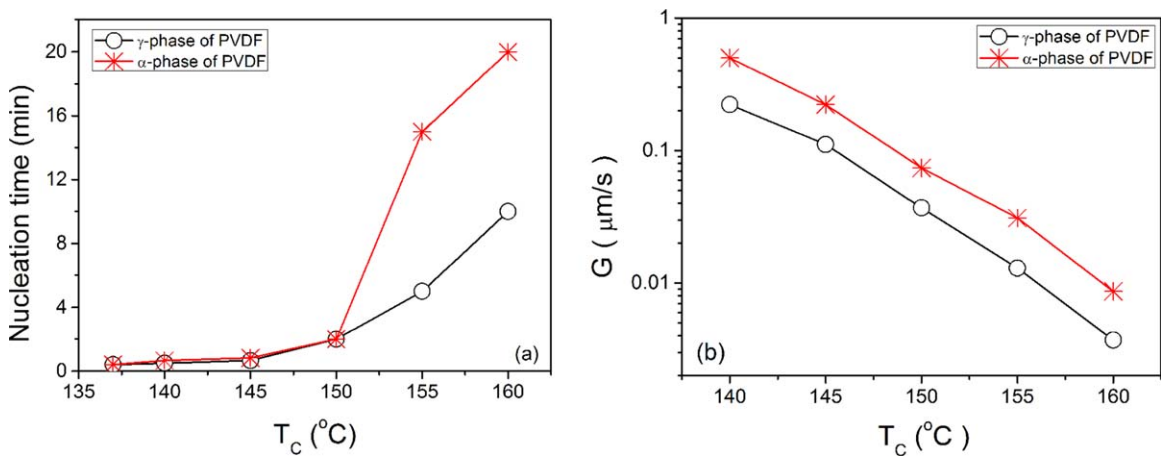

Figure 8. (a) The nucleation rate and (b) growth rate of α and γ phase spherulites of PVDF isothermally crystallized at different temperatures. [Color figure can be viewed in the online issue, which is available at wileyonlinelibrary.com.]

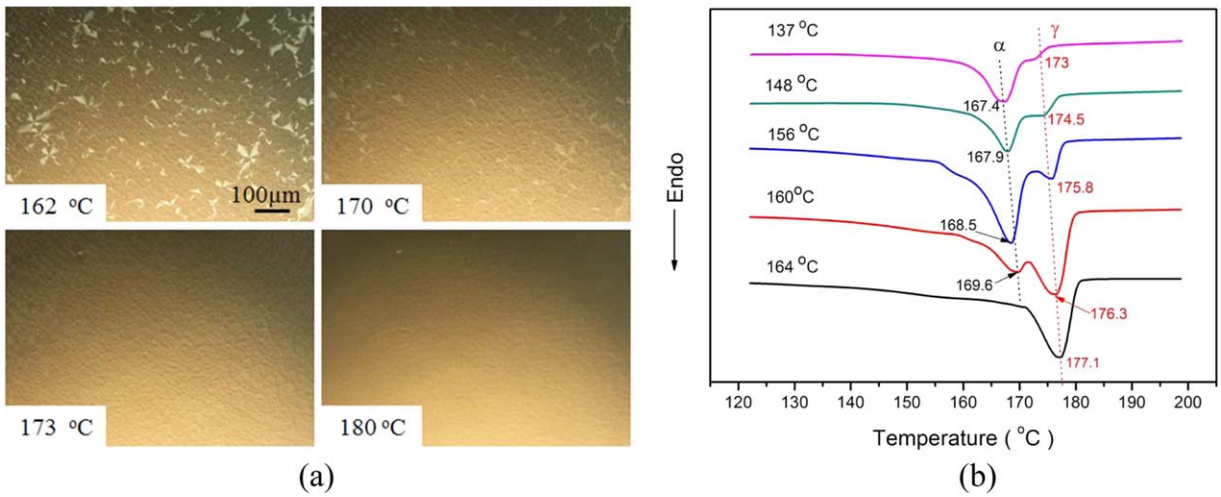

Figure 9. (a) POM images of melting process of PVDF crystals obtained after isothermal crystallization at 150 °C, (b) DSC thermograms of subsamples of neat PVDF selected from the T_c-crystal morphology library. [Color figure can be viewed in the online issue, which is available at wileyonlinelibrary.com.]

resulted in a more intense competition between the α and γ phase crystallization. Finally, γ phase crystallization was suppressed by α phase at 137 °C.

Different from Silvar *et al.*'s results,[23] γ phase could be observed at T_c as low as 140 °C in this work. A few α nuclei formed at the early stage of isothermal crystallization as shown in Figure 7(b–d). As time went by, a large amount of α nuclei emerged around the pre-existing γ nuclei. These α nuclei were induced by the γ nuclei, and their radii were much small than the α nuclei formed at the early stage of the crystallization. The promotion of PVDF γ phase to the nucleation of α phase observed in this particular study had not yet been reported in other literatures to our best of knowledge.

Figure 8(a,b) present the nucleation rate and growth rate of α and γ phase spherulites of PVDF isothermally crystallized at

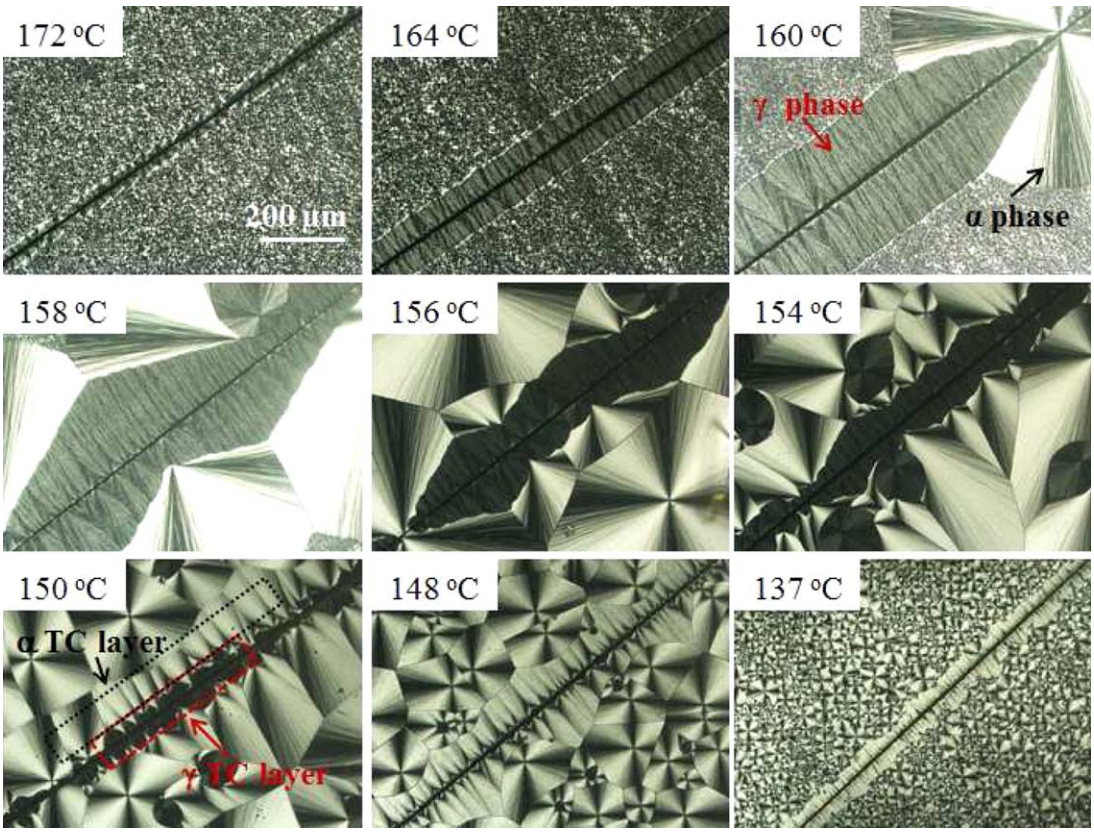

Figure 10. The POM images of TC structure in CF/PVDF composite after 4 h' isothermal crystallization on the T-gradient hot stage. [Color figure can be viewed in the online issue, which is available at wileyonlinelibrary.com.]

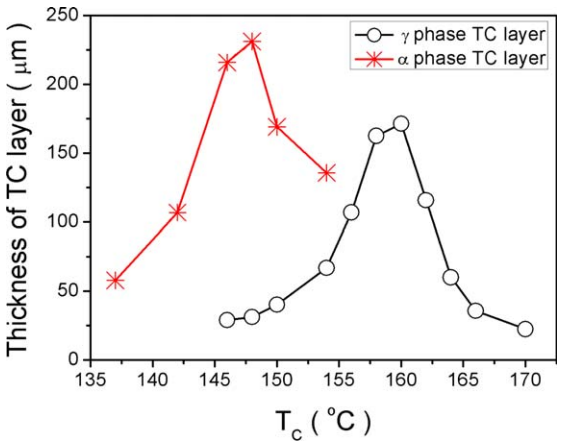

Figure 11. The thickness of γ phase and α phase TC layer in CF/PVDF composite film isothermally crystallized on the T-gradient. [Color figure can be viewed in the online issue, which is available at wileyonlinelibrary.com.]

different temperatures, respectively. Both the nucleation time of α and γ phase decreased with decreasing T_c. However, the nucleation time of γ phase was much shorter than that of the α phase when T_c was above 150 °C. It indicated that α phase has weaker nucleation ability than γ phase at high T_c as discussed above. The growth rate of both α and γ phase spherulites increased as T_c decreased, but the γ phase spherulite grew much slower than α phase at the same T_c.

PVDF crystals obtained after isothermal crystallization at 150 °C was melted on the hot stage and observed using POM as shown in Figure 9(a). It was known that the T_m of γ phase was higher than that of α phase.[6,23] α phase spheruites began to melt at about 170 °C, while γ phase spherulites did not melt until 180 °C. To confirm the content of α and γ crystalline phases, subsamples of neat PVDF crystallized at 164, 160, 156, 148, and 137 °C were selected from the T_c-crystal morphology library to conduct the DSC measurement.

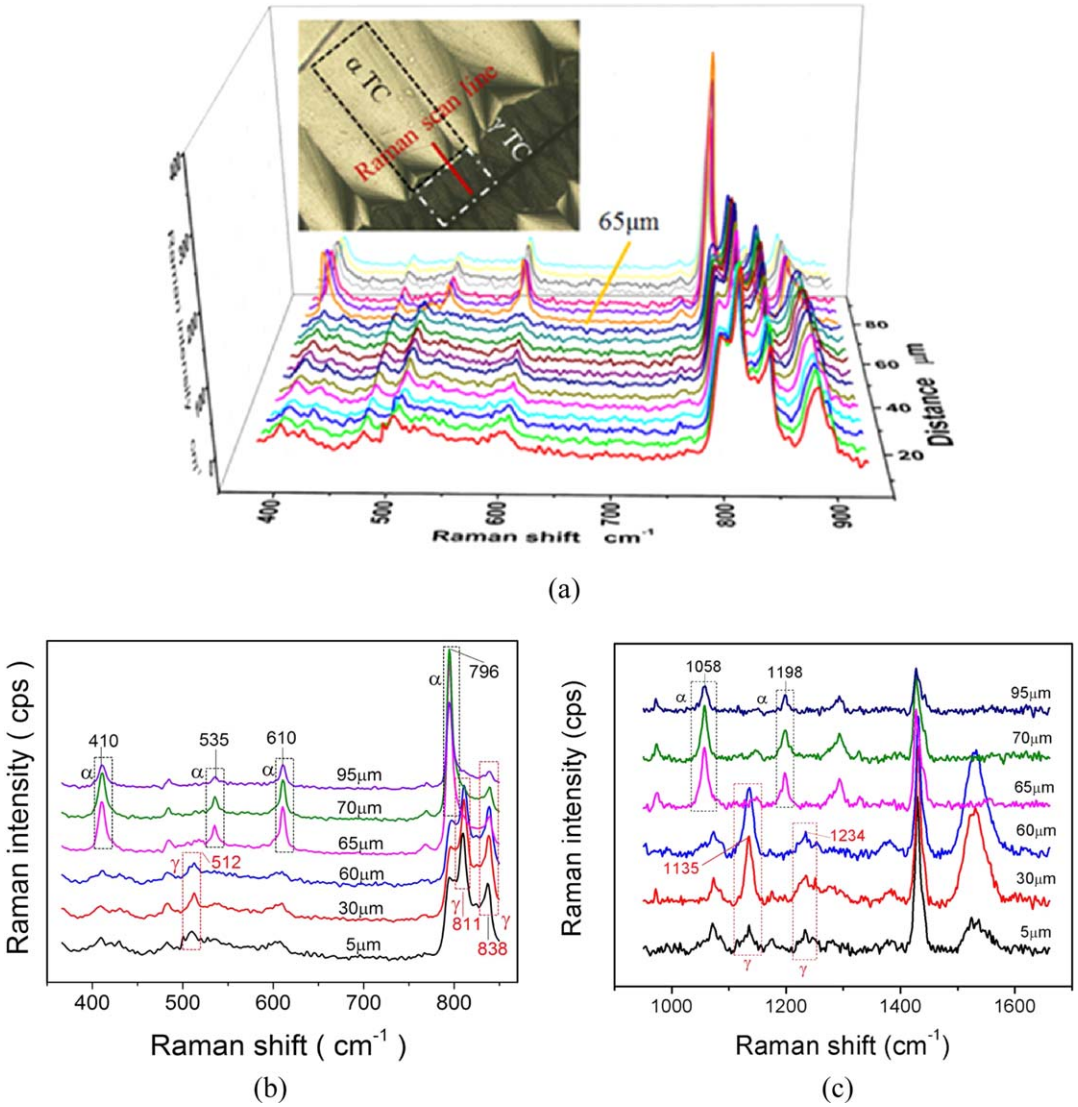

Figure 12. (a) The micro-Raman spectra of a doubled TC layers formed at 150 °C at different positions along the scan line. The selected micro-Raman spectra scanned at different positions along the scan line perpendicular to the CF long axis at (b) low Raman shift region (left) and (c) high Raman shift region (right). [Color figure can be viewed in the online issue, which is available at wileyonlinelibrary.com.]

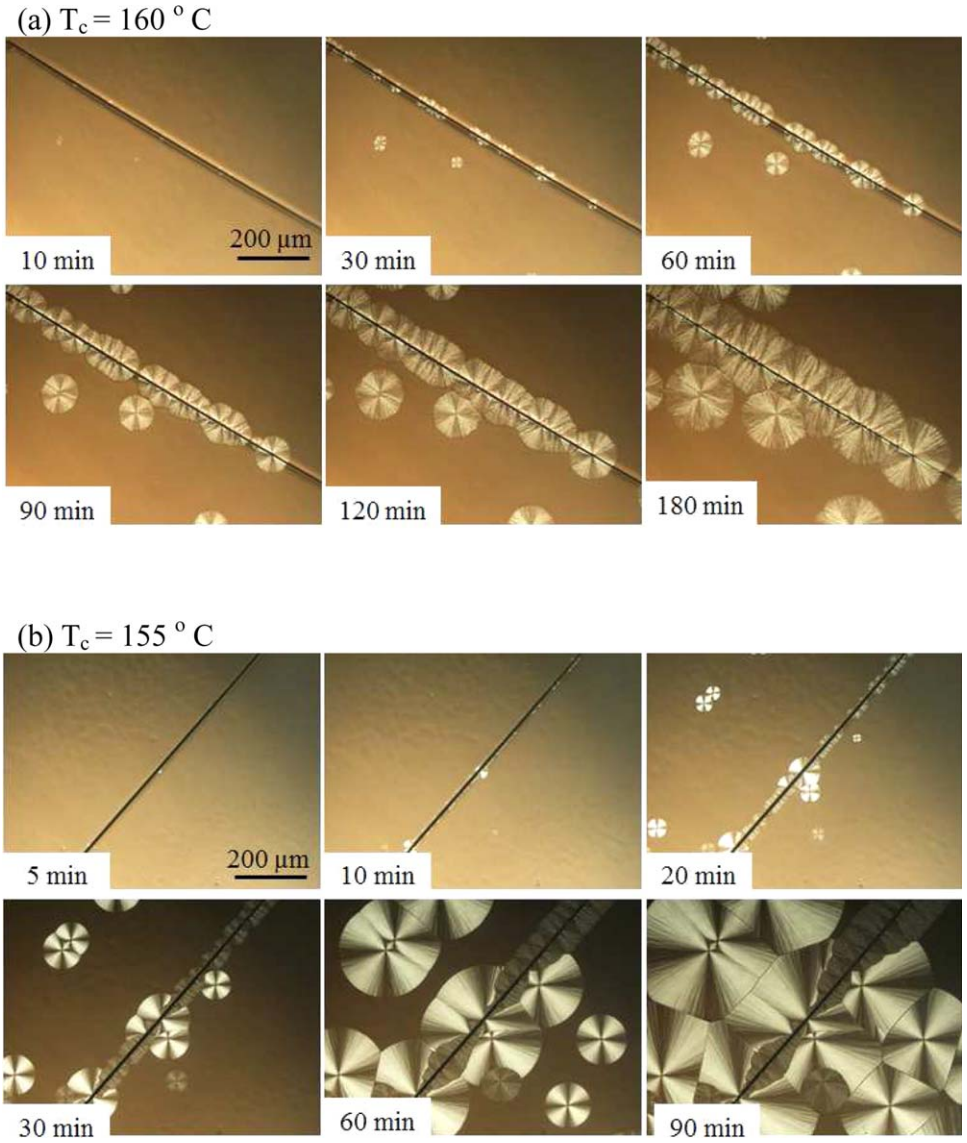

Figure 13. The POM images of CF/PVDF composite film isothermally crystallized at different temperatures. [Color figure can be viewed in the online issue, which is available at wileyonlinelibrary.com.]

As shown in Figure 9(b), the subsample crystallized at 164 °C presented only one melting peak in the heating program, which corresponded to the γ phase observed by POM in Figure 2. But two melting peaks were observed in the DSC thermograms of the subsamples crystallized at 160, 156, 148, and 137 °C. According to the POM observation in Figure 9(a), the melting peaks at higher temperatures (173–177 °C) corresponded to γ phase, and the peaks at lower temperatures (167–170 °C) corresponded to α phase. In the range of 164–137 °C, the content of γ phase decreased as T_c decreased according to the DSC curves, which was in agreement with FTIR and POM data.

Transcrystallization in CF/PVDF Composite

Figure 10 shows the POM images of TC structure in CF/PVDF composite after 4-h isothermal crystallization on the T-gradient stage. Only γ phase hybrid nucleation was found on the surface of CF when T_c was above 160 °C. In this case, TC layer was composed of exclusive γ phase. As T_c decreased, more and more α phase nuclei were found on the surface of CF. Nevertheless, hybrid nucleation on the surface of CF was still dominated by γ phase when T_c was in the range of 160–150 °C. Finally, γ phase nuclei were soon circumscribed by the rapidly developed α phase when T_c was below 144 °C. Therefore, the hybrid nucleation ability of γ phase on the surface of CF was much stronger than that of the α phase at high T_c. The hybird nucleation ability of α phase increased with the decreasing T_c, which resulted in a more intense competition between α and γ phase hybrid nucleation. Hence, the transcrystallization behavior of α and γ phase was very similar with that of the neat PVDF. Furthermore, the α phase TC layer was found around the γ phase TC layer when T_c was in the range of 146–156 °C. In other words, a doubled TC layer could form on the surface of CF. The outer α phase TC layers may be induced by γ phase just as it occurred in the case of the neat PVDF crystallization.

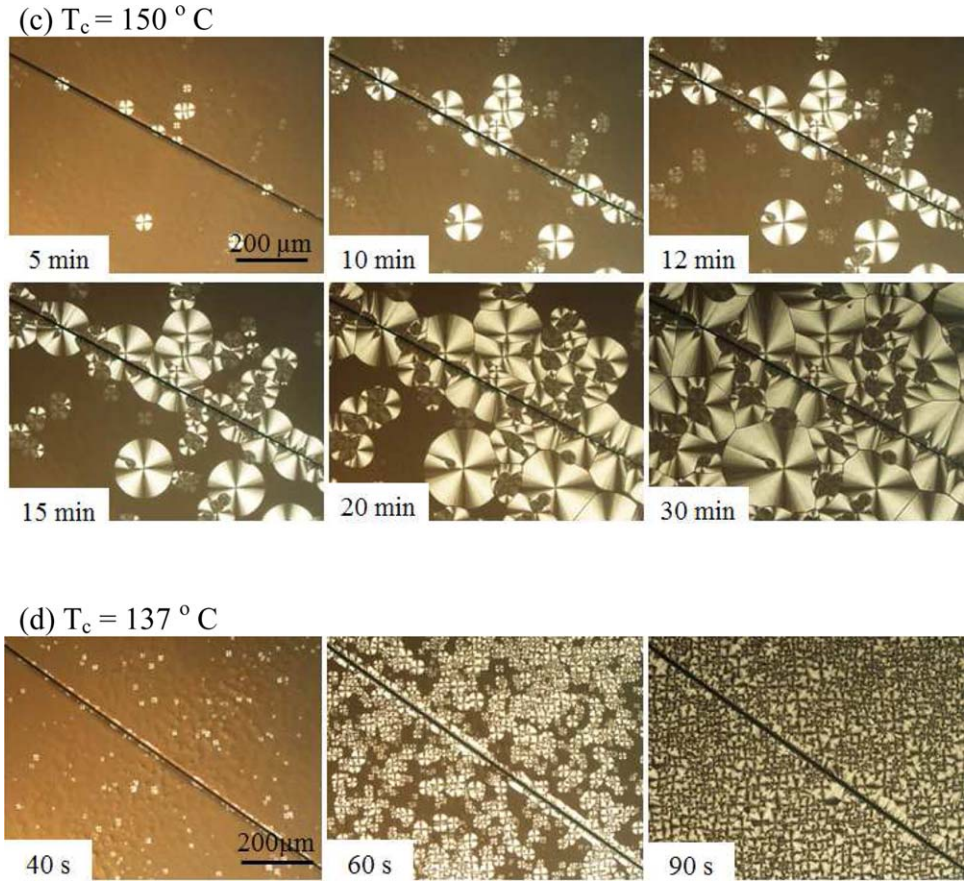

Figure 13. (*Continued*). [Color figure can be viewed in the online issue, which is available at wileyonlinelibrary.com.]

Figure 11 presents the thickness of γ phase TC layer and α phase TC layer (on the surface of γ phase) in the CF/PVDF composite crystallized isothermally on the T-gradient for 4 h. The thickness of γ phase reached its maximum at 160 °C. The α phase TC layer formed between 137 and 154 °C, and reached its maximum thickness at 148 °C. The thickness of the α phase TC layer was 75–200 μm larger than that of the γ phase TC layer at the same T_c.

To observe the transcrystallization in CF/PVDF composite at molecular level, micro-Raman measurement was conducted for the TC structure formed at 150 °C along a 90-μm line (5–95 μm away from the surface of CF) perpendicular to the long axis of the CF with a step size of 5 μm. The micro-Raman spectra are shown in Figure 12(a) with the schematic of the sample and scan line. As shown in Figure 12(a), the micro-Raman spectra collected at the position of 5 to 60 μm away from the surface of

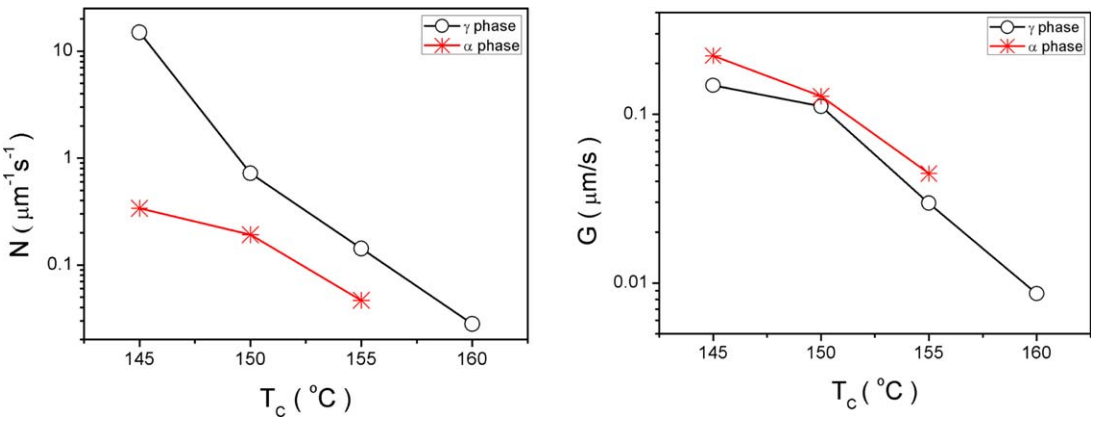

Figure 14. The nucleation rate and growth rate of α and γ phase on the surface of CF in CF/PVDF composites isothermally crystallized at different temperatures. [Color figure can be viewed in the online issue, which is available at wileyonlinelibrary.com.]

CF were essentionally the same. Whereas, at the position of 65- to 95-μm away from the surface of CF, the micro-Raman spectra showed no obvious differences.

Then, the micro-Raman spectra, which were scanned at the position of 5, 30, 60, 65, 70, and 95 μm away from the surface of CF, were selected and compared in Figure 12(b,c). The same as discussed in the micro-Raman measurement of neat PVDF, the bands at 512, 1135, and 1234 cm^{-1} corresponded to the γ phase TC layer. The bands at 283, 410, 535, 610, 1058, and 1198 cm^{-1} corresponded to the α phase TC layer. So the boundary of γ and α phase TC layers was in the range of 60–65 μm away from the surface of CF. No obvious shift of α phase characteristic band was observed in the spectra which were scanned at 65, 70, and 95 μm away from the surface of CF in this study. However, the band 811 cm^{-1} ($\gamma(CH_2)$) of PVDF γ phase in the spectrum obtained at the position of 30 μm shifted more than 1 cm^{-1} to the high wavenumber region compared with the spectrum at the position of 5 μm. This shift might be attributed to the interaction between PVDF molecules of γ phase TC layer and CF surface.[27,28]

Kinetics of Transcrystallization in CF/PVDF Composite

Figure 13 shows the POM images of transcrystallization in CF/PVDF composite during isothermal crystallization at 160, 155, 150, 145 and 137 °C. Exclusive γ phase nuclei formed on the surface of CF at 160 °C, and finally developed into a cylindrical TC layer as shown in Figure 13(a). Furthermore, the nucleation rate on the surface of CF was much faster than that in the bulk matrix. At $T_c = 155$ °C as shown in Figure 13(b), a few α phase nuclei emerged on the surface of CF, but hybrid nucleation was still dominated by γ phase. However, the α phase nuclei grew very fast and soon surrounded the γ phase nuclei. As T_c decreased to 150 °C, many α phase nuclei were induced at the surface of the γ phase TC layer, and finally developed into α phase TC layer, which resulted in a doubled TC layer at the interface of CF and PVDF matrix. The transition from γ phase to α phase also occurred in the bulk matrix, which was in agreement with crystallization of neat PVDF at 150 °C. On one hand, competition between hybrid nucleation of α and γ phase on the surface of CF became more intense as T_c decreased. As T_c decreased to 137 °C, hybrid nucleation on the surface of CF was dominated by α phase. On the other hand, there was competion between the transcrystallization and homogenous crystallization in the bulk matrix,[5,18] which became more intense as T_c decreased. Thus, the thickness of TC layer was significanly influenced by T_c.

Figure 14 shows the nucleation rate and growth rate of α and γ phase on the surface of CF at T_c in the range of 145–160 °C. As indicated in Figure 14, the hybrid nucleation rate of both α and γ phase on the surface of CF increased with decreasing T_c. However, the hybrid nucleation rate of γ phase was much higher than that of α phase at the same T_c. Both the growth rate of α and γ phase TC layers increased as T_c decreased. But the growth rate of α phase TC layer was higher than that of γ phase at the same T_c. Hence, the dependence of transcrystallization kinetics on T_c was similar with crystallization of neat PVDF. As it was shown in Figure 8(a), the nucleation rate of α phase was lower than γ phase of the neat PVDF at the T_c higher than 145 °C. Meanwhile, the growth rate (G) of α phase spherulite was higher than that of γ phase of the neat PVDF at the T_c between 145 and 155 °C.

CONCLUSIONS

The influence of T_c on crystallization behavior of PVDF and CF/PVDF composite films was investigated using a controlled T-gradient hot stage. For neat PVDF, both α and γ phase spherulites were observed at T_c ranging from 137 to 160 °C. It was different from the previous reported results that γ phase could only be obtained at T_c above 160 °C. Most importantly, α phase nuclei were observed around γ phase spherulites for the first time. For CF/PVDF composite, the cylindrical TC layer formed on the surface of CF when T_c was in the range of 137–172 °C. Some α phase nuclei were induced at the surface of γ phase TC layer when T_c was in the range of 146–156 °C, which finally developed into a unique doubled TC layer with γ phase at the interface of the composite.

ACKNOWLEDGMENTS

The authors gratefully thank the financial support from the National Natural Science Foundation of China (Grants: 20774014, 21074016).

REFERENCES

1. Nalwa, H. S. In Ferroelectric Polymers: Chemistry, Physics, and Applications; Nalwa, H. S., Ed.; Marcel Dekker, Inc: New York, **1995** p 67.
2. Lovinger, A. *J. Sci.* **1983**, *220*, 1115.
3. Hasegawa, R.; Kobayashi, M.; Tadokoro, H. *Polym. J.* **1972**, *3*, 591.
4. Hasegawa, R.; Takahashi, Y.; Chatani, Y.; Tadokoro, H. *Polym. J.* **1971**, *3*, 600.
5. Davis, G. T.; McKinney, J. E.; Broadhurst, M. G.; Roth, S. C. *J. Appl. Phys.* **1978**, *49*, 4998.
6. Tashiro, K.; Tadokoro, H.; Kobayashi, M. *Ferroelectrics* **1981**, *32*, 167.
7. Park, S. J. Carbon Fibers; Springer: Dordrecht, **2015**.
8. Ram, R.; Rahaman, M.; Khastgir, D. *J. Appl. Polym. Sci.* **2014**, *131*, DOI: 10.1002/app.39866.
9. Wang, J.; Wu, D.; Li, X.; Zhang, M.; Zhou, W. *Appl. Surf. Sci.* **2012**, *258*, 9570.
10. Thomason, J. L.; Van Rooyen, A. A. *J. Mater. Sci.* **1992**, *27*, 889.
11. Thomason, J. L.; Van Rooyen, A. A. *J. Mater. Sci.* **1992**, *27*, 897.
12. Sukhanova, T. E.; Lednický, F.; Urban, J.; Baklagina, Y. G.; Mikhailov, G. M.; Kudryavtsev, V. V. *J. Mater. Sci.* **1995**, *30*, 2201.
13. Heppenstall-Butler, M.; Bannister, D. J.; Young, R. *J. Compos. Part A: Appl. Sci. Manuf.* **1996**, *27*, 833.

14. Ning, N.; Fu, S.; Zhang, W.; Chen, F.; Wang, K.; Deng, H.; Zhang, Q.; Fu, Q. *Prog. Polym. Sci.* **2012**, *37*, 1425.
15. Karger-Kocsis, J. *Adv. Compos. Lett.* **2000**, *9*, 225.
16. Wu, C. M.; Chen, M.; Karger-Kocsis, J. *Polymer* **1999**, *40*, 4195.
17. Cho, K.; Kim, D.; Yoon, S. *Macromolecules* **2003**, *36*, 7652.
18. Xu, H.; Xie, L.; Jiang, X.; Li, X.; Li, Y.; Zhang, Z.; Zhong, G.; Li, Z. *J. Phys. Chem. B* **2014**, *118*, 812.
19. Varga, J.; Karger-Kocsis, J. *Compos. Sci. Technol.* **1993**, *48*, 191.
20. Varga, J.; Karger-Kocsis, J. *J. Mater. Sci. Lett.* **1994**, *13*, 1069.
21. Cai, Y.; Petermann, J.; Wittich, H. *J. Appl. Polym. Sci.* **1997**, *65*, 67.
22. Xu, D.; Bin, Y.; Tang, P. *Macromolecules* **2010**, *43*, 5323.
23. Silva, M. P.; Sencadas, V.; Botelho, G.; Machado, A. V.; Rolo, A. G.; Rocha, J. G.; Lanceros-Mendez, S. *Mater. Chem. Phys.* **2010**, *122*, 87.
24. Tashiro, K.; Kobayashi, M.; Tadokoro, H. *Macromolecules* **1981**, *14*, 1757.
25. Kobayashi, M.; Tashiro, K.; Tadokoro, H. *Macromolecules* **1975**, *8*, 158.
26. Benz, M.; Euler, W.; Gregory, O. *Macromolecules* **2002**, *35*, 2682.
27. Zhao, Q.; Wagner, H. D. *Philos. Trans. A. Math. Phys. Eng. Sci.* **2004**, *362*, 2407.
28. Qi, H.; Liu, J.; Mäder, E. *Fibers* **2014**, *2*, 295.